Bull Volcanol (1989) 51:88-95

Bulletin of
Volcanology

© Springer-Verlag 1989

A dynamical model of lava flows cooling by radiation

Michele Dragoni

Dipartimento di Fisica, Università di Bologna, Viale Berti Pichat 8, I-40127 Bologna, Italy

Abstract. The behaviour of a lava flow is reproduced by a two-dimensional model of a Bingham liquid flowing down a uniform slope. Such a liquid is described by two rheological parameters, yield stress and viscosity, both of which are strongly temperature-dependent. Assuming a flow rate and an initial temperature of the liquid at the eruption vent, the temperature decrease due to heat radiation and the consequent change in the rheological parameters are computed along the flow. Both full thermal mixing and thermal unmixing are considered. The equations of motion are solved analytically in the approximation of a slow downslope change of the flow parameters. Flow height and velocity are obtained as functions of the distance from the eruption vent; the time required for a liquid element to reach a certain distance from the vent is also computed. The gross features of observed lava flows are reproduced by the model which allows us to estimate the sensitivity of flow dynamics to changes in the initial conditions, ground slope and rheological parameters. A pronounced increase in the rate of height increase and velocity decrease is found when the flow enters the Bingham regime. The results confirm the observation according to which lava flows show an initial rapid advance, followed by a marked deceleration, while the final length of a flow is such that the Graetz number is in the order of a few hundreds.

Introduction

In Newtonian viscous fluids, the strain rate is proportional to the applied shear stress. Lava shows instead a non Newtonian behaviour, in that lava flows construct their levées by themselves and may come to rest on a slope. It was proposed by Robson (1967) that the rheology of lava is approximately that of a Bingham liquid (or plastic), which is characterized by a yield stress. If the applied stress is less than the yield value, no permanent strain is produced. The Bingham plastic model was able to explain the relation found by Walker (1967) between flow thickness and ground slope on Mt. Etna and the characteristics of debris and mud flows (Johnson 1970). The existence of a yield stress in basaltic lava was assessed by Shaw et al. (1968). Hulme (1974) explained the morphology of lava flows on the basis of the Bingham plastic model. The model has been supported by observations of lava flows moving downslope (Borgia et al. 1983).

An important point is that both yield stress and viscosity are strongly temperature-dependent (Johnson and Pollard 1973; Pinkerton and Sparks 1978; Spera et al. 1982). This has a great effect on the behaviour of lava flows. Cooling is in fact an important factor in limiting the downslope flow of lava (Wadge 1978). Once the lava leaves the eruption vent and flows downhill, it begins to cool and a thermal boundary layer develops at the surfaces of the flow. This has the effect of reducing the heat loss: therefore the temperature gradient along the flow is small. Isothermal models of lava flows are therefore a reasonable approximation in describing a limited segment of flow, where temperature can be considered as uniform (Dragoni et al. 1986).

In the present paper, cooling of the flow is taken into account. Of the various processes of heat loss, conduction to the atmosphere is negligible. Convection in the atmosphere is responsible for a part of heat loss, but numerical estimates indicate that its contribution is much smaller than that due to black body radiation (Murase and

McBirney 1970; Daneš 1972). As to the effect of conduction to the ground, it has been shown (Hulme 1982) that flow lengths are generally much less than the distances at which this contribution to cooling can significantly affect the flow. Moreover, most of the heat generated by dissipation will be transferred to the ground, since in a Bingham liquid shearing takes place in a thin layer close to the base of the flow. Degassing has a significant effect on the temperature and the rheology of lava (Scarfe 1973; Sparks and Pinkerton 1978): this effect is mostly important in the early stages of flow and is probably responsible for a drastic change in the rheology of magma before eruption to that of flowing lava.

Accordingly, in the present paper, only heat loss by radiation is considered. A model is proposed which describes the downslope flow of an incompressible Bingham plastic cooling by radiation. Two cases are considered: full thermal mixing in the flow and thermal unmixing (Pieri and Baloga 1986). The steady-state laminar-flow solution of the Navier-Stokes equation is obtained analytically and the downslope evolution of the rheological and dynamical parameters of the flow is studied. On the basis of a similar model, Park and Iversen (1984) worked out by a numerical method the thickness growth of a downslope, thermally mixed lava flow.

The model considers flow well behind the flow front. In that zone the levées can be taken as fixed, since they are cooler and have a higher yield stress than fresh lava flowing between them (Sparks et al. 1976). Therefore, processes at the front, including levée formation, the change in shape of the flow and the choice of flow path, are not taken into account. The model, being two-dimensional, neglects friction at the levées. It is therefore appropriate to low aspect ratio flows. The aspect ratio is defined as the ratio of flow height to flow width (Hulme 1974). It has been observed in the field that lavas with low values of yield stress, such as basalts, produce flows of low aspect ratio ($\ll 1$), while more acidic lavas produce flows with higher aspect ratios, but usually always less than 1 (Walker 1973).

The model

We consider the stationary downslope flow of a Bingham liquid (Fig. 1). The flow occurs in the x direction, while no changes in the flow are considered in the y direction. The liquid has density ρ

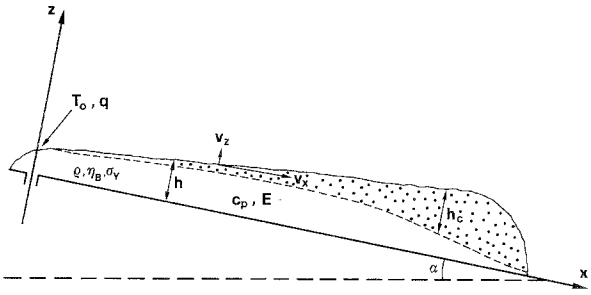

Fig. 1. The model: a downslope section of lava flow is shown with the coordinate system and the relevant parameters

and viscosity η. It is assumed to be incompressible:

$$\frac{\partial v_x}{\partial x} + \frac{\partial v_z}{\partial z} = 0 \tag{1}$$

where $\mathrm{v} = (v_x, 0, v_z)$ is the velocity vector and both v_x and v_z depend on x and z, since the liquid will be allowed to change its height along the flow. The equation of motion is the two-dimensional steady-state Navier-Stokes equation, where the nonlinear terms are dropped since we are considering a low-velocity flow (creeping approximation). We shall be interested in the x-component of this equation, which for variable viscosity reads (Landau and Lifchitz 1971):

$$2\frac{\partial}{\partial x}\left(\eta \frac{\partial v_x}{\partial x}\right) + \frac{\partial}{\partial z}\left[\eta\left(\frac{\partial v_x}{\partial z} + \frac{\partial v_z}{\partial x}\right)\right] + \rho g \sin\alpha = 0 \tag{2}$$

where g is the acceleration of gravity and α is the slope of the ground.

We make two assumptions: (1) the change of velocity along the flow is much slower than the change with depth z; (2) viscosity is constant with depth in each vertical cross section of the flow. Accordingly, Eq. (2) reduces to the lubrication theory approximation, which is commonly employed in similar problems (Huppert 1982; Emerman and Turcotte 1983):

$$\eta(x)\, \partial^2 v_x/\partial z^2 + \rho g \sin\alpha = 0. \tag{3}$$

Boundary conditions for Eq. (3) are $v_x = 0$ at $z = 0$ and vanishing traction at the free surface of the flow, $z = h(x)$.

Assumption (2) above is of course a crude approximation of actual lava flows, where temperature varies as a function of z, entailing a corresponding change in the rheological parameters. In

particular, one may argue that the viscosity gradient $\partial\eta/\partial z$, which has been neglected in writing Eq. (3), reaches significant values within the flow. However, these high values are mainly confined to the thermal boundary layer which develops at the surface of the flow, where the temperature gradient is highest; deeper in the flow, temperature can be considered as constant to a good approximation (e.g. Archambault and Tanguy 1976, for field measurements). But the *rheological* boundary layer is always much thinner than the *velocity* boundary layer (i.e. the plug) characterizing Bingham liquids (Hulme 1982), so that the highest values of $\partial\eta/\partial z$ take place within the plug: therefore, neglecting $\partial\eta/\partial z$ in Eq. (2) will not have finally a large effect on the flow dynamics.

The presence of a thermal boundary layer will have a larger effect on the heat loss of the flow. In a thermally mixed flow, the equation of heat loss due to radiation is given, at constant flow rate, by (e.g. Daneš 1972; Park and Iversen 1984):

$$c_p q \frac{dT}{dx} + E\Sigma T^4 = 0 \tag{4}$$

where c_p is the specific heat, q is the mass flow rate per unit width, E is the emissivity and Σ is the Stefan constant. The solution of Eq. (4) is easily found to be:

$$T(x) = T_0 \left(\frac{3E\Sigma T_0^3}{c_p} \frac{x}{q} + 1 \right)^{-1/3} \tag{5}$$

where T_0 is the temperature at $x=0$ (the eruption vent). Equation (4) implies that temperature is constant in each vertical cross section of the flow and that the local radiative loss is characteristic of that temperature. Pieri and Baloga (1986) suggested that the presence of a cooler crust on the flow can be taken into account by assuming that radiative heat loss takes place at an effective temperature T_e, which is smaller than the temperature of the interior of the flow. In this 'thermally unmixed' case, the heat equation would be:

$$c_p q \frac{dT}{dx} + E\Sigma T_e^4 = 0 \tag{6}$$

where T_e is a constant. The solution of Eq. (6) is:

$$T(x) = T_0 - \frac{E\Sigma T_e^4}{c_p} \frac{x}{q}. \tag{7}$$

Both cases, Eqs. (4) and (6), will be considered in the present model.

The constitutive relation of a Bingham liquid is characterized by a yield stress σ_γ (e.g. Skelland 1967):

$$\dot{\varepsilon} = \begin{cases} 0, & \sigma < \sigma_\gamma \\ (\sigma - \sigma_\gamma)/\eta_B, & \sigma > \sigma_\gamma \end{cases} \tag{8}$$

where σ is the maximum deviatoric stress, $\dot{\varepsilon}$ is the corresponding strain rate and η_B is the Bingham viscosity. In our case, $\dot{\varepsilon} = \partial v_x/\partial z$. Since temperature is allowed to change along the flow, we must introduce laws relating temperature T to rheological parameters η_B and σ_γ. As to viscosity, we assume the following relation (e.g. Shaw 1969; Pinkerton and Sparks 1978; Spera et al. 1982):

$$\eta_B(T) = \eta_l e^{a(T_l - T)}, \quad T < T_l \tag{9}$$

where T_l is the liquidus temperature, η_l is the viscosity at temperature T_l and a is a parameter. The analytical dependence of σ_γ on temperature is more uncertain: σ_γ is zero at the liquidus temperature, increasing exponentially below T_l. For the sake of simplicity we assume for $\sigma_\gamma(T)$ a relationship similar to Eq. (9):

$$\sigma_\gamma(T) = \sigma_{\gamma 0}[e^{b(T_l - T)} - 1] \tag{10}$$

which, with appropriate values of the parameters $\sigma_{\gamma 0}$ and b, can reproduce the order-of-magnitude changes of yield stress measured by some authors (Robson 1967; Pinkerton and Sparks 1978; McBirney and Noyes 1979) in limited temperature ranges. Equations (9) and (10) are not meant to describe the rheology of a particular lava, but simply to find out the effect of these strongly temperature-dependent parameters on lava flow dynamics.

The above-written equations are now used to obtain the flow dynamics at a point x downslope. Temperature $T(x)$ is computed from Eqs. (5) or (7) and the rheological parameters are then computed according to Eqs. (9) and (10). Equations (3) and (8) yield then (Johnson 1970):

$$v_x(x, z) =$$

$$\frac{1}{2\eta_B} \begin{cases} \rho g \sin\alpha \; z(2h - z) - 2\sigma_\gamma z, & 0 < z < h - h_c \quad (11a) \\ \rho g \sin\alpha \; h^2 (1 - \sigma_\gamma/\sigma_b)^2, & h - h_c < z < h \quad (11b) \end{cases}$$

where:

$$\sigma_b(x) = \rho g h \sin\alpha \tag{12}$$

is the shear stress at the base of the flow and:

$$h_c(x) = \sigma_\gamma/(\rho g \sin\alpha) \tag{13}$$

is the critical height of the flow, e.g. the thickness of the undeformed part of the flow (the plug) where the shear stress is less than σ_γ. The flow velocity v_x is related to the flow rate q, per unit width of the flow, by:

$$q = \rho \int_0^{h(x)} v_x(x,z)\, dz. \tag{14}$$

The knowledge of v_x as given by Eq. (11) allows one to obtain from Eq. (14) an equation relating the flow height h to the model parameters (Skelland 1967; Hulme 1974):

$$\left(\frac{h}{h_c}\right)^3 - \frac{3}{2}\left(\frac{h}{h_c}\right)^2 - \frac{3\eta_B q}{\rho\sigma_\gamma h_c^2} + \frac{1}{2} = 0. \tag{15}$$

The height $h(x)$ is obtained analytically as a solution of Eq. (15) (see Dragoni et al. 1986). Then v_x is obtained from Eq. (11), while v_z is:

$$v_z(x) \simeq v_x \frac{dh}{dx} \tag{16}$$

The time $t(x)$ required for an element of liquid to flow a distance x from the origin is computed as:

$$t(x) = \int_0^x \frac{dx'}{v_x(x')} \tag{17}$$

which will be called 'flow time'. Finally, the Graetz number Gz is computed along the flow:

$$Gz(x) = v_0 h_0^2/(Kx) \tag{18}$$

where v_0 and h_0 are the flow velocity and height at $x=0$, respectively; K is the thermal diffusivity. The Graetz number is a dimensionless quantity which measures the extent to which a channelled liquid is close to solidification due to heat loss. There is theoretical and observational evidence that flow ceases when Gz has decreased from an initially large value to a few hundred (Pinkerton and Sparks 1976; Hulme and Fielder 1977).

It is interesting to note that the temperature T in Eqs. (5) and (7) depends on the ratio x/q between distance from the vent and flow rate density. Consequently, the same holds for the rheological parameters σ_γ and η_B, flow height and velocity, flow time and Graetz number. It is therefore useful to plot these quantities as functions of x/q in describing the flow behaviour.

The dynamical parameters of flow are calculated assuming a fixed flow rate per unit width q along the flow. This is equivalent to fix the flow rate Q (i.e. the effusion rate) and the flow width w:

$$q = Q/w \tag{19}$$

Observations show in fact that, after flowing a short distance, the lava motion occurs in a channel contained between stationary levées.

Numerical examples

A typical flow dynamics according to this model is computed by using the numerical values listed in Table 1 for the model parameters. Such values are meant to represent a basaltic lava flow. An initial temperature $T_0 = T_l = 1200\,^\circ$C is assumed at the eruption vent ($x=0$). However, all graphs can be read for any lower initial temperature: to this aim it is sufficient to read the graphs starting from the point on each curve which corresponds to the chosen temperature value and shifting correspondingly the zero of the abscissa scale.

As lava radiates heat into the atmosphere, its temperature decreases as is shown in Fig. 2 as a function of x/q. The curve for the unmixed case has been drawn by assuming $T_e = 900\,^\circ$C, which is

Table 1. Values of the model parameters which have been used in drawing the graphs. The values for E, c_p and K are currently employed for lavas (Hulme 1982; Wilson and Head 1983; Park and Iversen 1984). The values taken for η_l, $\sigma_{\gamma 0}$, a and b reproduce a possible temperature dependence for basaltic magmas (Pinkerton and Sparks 1978; McBirney and Noyes 1979; McBirney and Murase 1984)

ρ	$=3000$ kg m^{-3}	Mass density
g	$=9.80$ m s^{-2}	Acceleration of gravity
α	$=0.20$ rad $\simeq 11.5^\circ$	Slope
T_0	$=1200\,^\circ$C	Initial temperature
E	$=0.6$	Emissivity
Σ	$=5.67\times10^{-8}$ J s^{-1} m^{-2} °K^{-4}	Stefan constant
c_p	$=8.37\times10^{2}$ J kg^{-1} °K^{-1}	Specific heat
K	$=3\times10^{-7}$ m^2 s^{-1}	Thermal diffusivity
η_l	$=10^2$ Pa s	Viscosity at $T=T_l$
a	$=0.04\,^\circ$K^{-1}	Parameter in $\eta_B(T)$
$\sigma_{\gamma 0}$	$=10^{-2}$ Pa	Parameter in $\sigma_\gamma(T)$
b	$=0.08\,^\circ$K^{-1}	Parameter in $\sigma_\gamma(T)$
T_l	$=1200\,^\circ$C	Liquids temperature
T_e	$=900\,^\circ$C	Effective radiation temperature

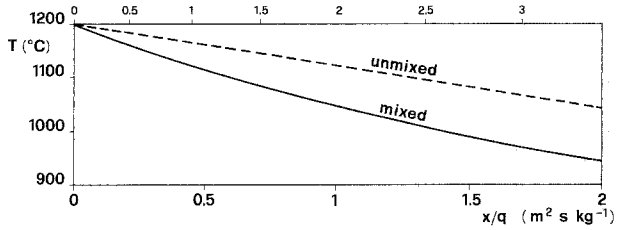

Fig. 2. Temperature T along the flow, as a function of the parameter x/q, for the thermally mixed case and the thermally unmixed case with $T_e = 900°C$ (lower horizontal scale). The *solid curve* represents also the unmixed case if the values of x/q are read on the upper horizontal scale. Initial temperature $T_0 = T_l = 1200°C$ is assumed

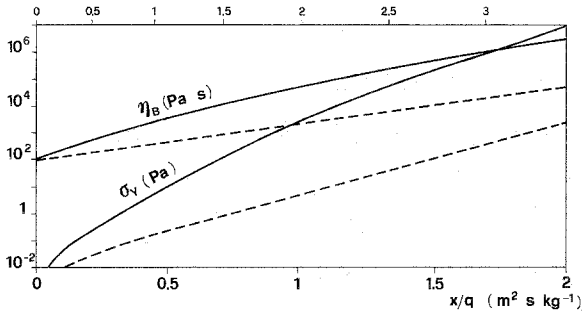

Fig. 3. Yield stress σ_γ and viscosity η_B along the flow, as functions of the parameter x/q, for the thermally mixed *(solid curves)* and the thermally unmixed *(dashed curves)* cases. *Solid curves* represent also the unmixed case if values of x/q are read on the upper horizontal scale

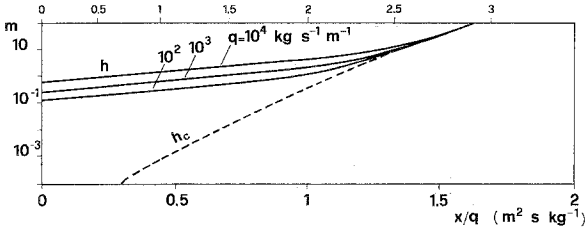

Fig. 4. Flow height h as a function of x/q, for three different values of flow rate q. The *dashed curve* is the critical height h_c. The lower and upper horizontal scales refer to the thermally mixed case and to the thermally unmixed case with $T_e = 900°C$, respectively

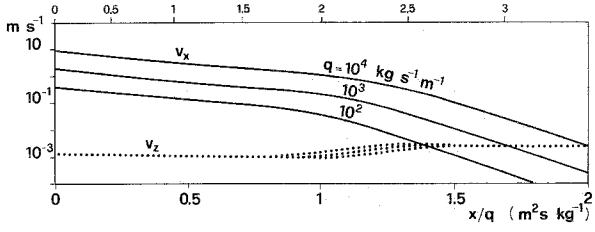

Fig. 5. Flow velocity components v_x *(solid curves)* and v_z *(dashed curves)*, as functions of x/q, for three different values of flow rate q. The lower and upper horizontal scales refer to the thermally mixed case and to the thermally unmixed case with $T_e = 900°C$, respectively

the upper bound of the temperature range considered by Pieri and Baloga (1986) and is close to the solidus temperature of basaltic lavas. This choice for T_e has been made simply to show the gross features of the flow behaviour in thermally unmixed conditions: any lower value for T_e would further reduce the temperature decrease along the flow. For instance, in the mixed case, a temperature $T_1 = 1000°C$ is reached at about 140 m from the vent if $q = 10^2$ kg s^{-1} m^{-1}, which represents a small lava flow: e.g. a flow of width $w = 1$ m, with volume flow rate $Q/\rho \cong 0.03$ m^3 s^{-1}. At the other extreme, T_1 is reached at $x = 14$ km if $q = 10^4$ kg s^{-1} m^{-1}, representing a large flow: e.g. $w = 10\,m$ and volume flow rate equal to $\sim 30\,m^3\,s^{-1}$. The corresponding values of x for the unmixed case are 260 m and 26 km.

If we assume that a flow stops when temperature at the front has fallen to a given value, independently of flow rate, the model shows that flow distance L may be proportional to the flow rate density q rather than to the effusion rate Q (Wadge 1978). Actually different conclusions have been reached by the observation of lava flows (Walker 1973; Malin 1980). There is a more complex relationship between Q and L, involving the lateral spreading of flows and, basically, the rheological properties of lavas (e.g. Baloga and Pieri 1986).

The corresponding change in the rheological parameters η_B and σ_γ is shown in Fig. 3. Both parameters increase by orders of magnitude along the flow. Values of σ_γ in the order of 10^5 Pa have been observed in the final stages of solidification (Robson 1967).

Figures 4 and 5 show respectively flow heights and velocity components as functions of x/q, for different values of flow rate density q. In these and the following graphs, the lower and upper horizontal scales refer to the thermally mixed case and to the thermally unmixed case with $T_e = 900°C$, respectively. At high temperatures, close to the liquidus, the flow is still in the Newtonian regime. Flow heights increase exponentially and flow velocities decrease exponentially as temperature decreases. As the flow cools, its height approaches the critical height h_c. With the model parameters of Table 1, the flow height is about 10 m when $T = T_1$; this happens at different distances from the vent according to the flow rate and to the thermal conditions (mixed or unmixed). A remarkable increase in the rate of

height increase occurs at $x/q > 1\ m^2\ s\ kg^{-1}$ for the mixed case and at $x/q > 2\ m^2\ s\ kg^{-1}$ for the unmixed case (note that the vertical scale is logarithmic). This height increase corresponds to a strong deceleration in the lava motion, which can be seen in Fig. 5, and indicates that the effect of the Bingham rheology becomes evident. Note that v_z is much smaller than v_x as long as the lava is flowing and $\partial v_z/\partial x \ll \partial v_x/\partial x$, according to the model assumptions.

In Fig. 6 a distance is considered downslope from the eruption vent, which is 1000 m for the thermally mixed case and about 2000 m for the thermally unmixed case. For both cases, three temperature curves are shown in Fig. 6(a) pertaining to different flow rates; the corresponding flow heights are shown in (b). This figure contains no more information than Figs. 2 and 4, but it makes clearer some features of a cooling flow. While the smallest flow ($q = 10^2\ kg\ s^{-1}\ m^{-1}$) cools down very rapidly and stops, the other two flows move through the whole distance considered in the graphs. An interesting fact can be noted in Fig. 6(b) which was not evident from Fig. 4: near to the eruption vent, larger flows are higher, but this is no longer true downslope. Considering the thermally mixed case, after less than 100 m, the smallest flow is already higher than the others, while at $x \simeq 400$ m the largest flow is the lowest; the corresponding values for the unmixed case are 200 m and 900 m. The model confirms the possibility of reproducing the paradoxical phenomenon proposed by Hulme (1974), where an increase in effusion rate leads to a decrease in flow height in a channel of fixed width. An increase in the effusion rate produces in fact a temperature increase at a given point along the flow (Fig. 6a): at a certain distance from the vent, this can correspond to a remarkable decrease in flow height (Fig. 6b).

The flow time, as defined by Eq. (17), is shown in Fig. 7 as a function of x/q and for different values of the flow rate density. For an easier comparison with field observations, x is plotted as a function of t in a graph with linear scales (Fig. 8) for some medium-size flow rates. It can be seen that the flow is very fast at the beginning and then drastically slows down. A different choice of the parameters entering the rheological laws Eqs. (9) and (10) would not sensibly alter this feature. A milder slope of the ground, as well as a lower initial temperature T_0, would have the effect of somewhat slowing the flow. The distance covered as a function of time is very sensitive to flow rate. Due to temperature decrease, the smaller flows in Fig. 8 will come to rest long before the 5-day span shown in the graph has elapsed. A comparison between the thermally mixed (left vertical scale) and the thermally unmixed case (right scale)

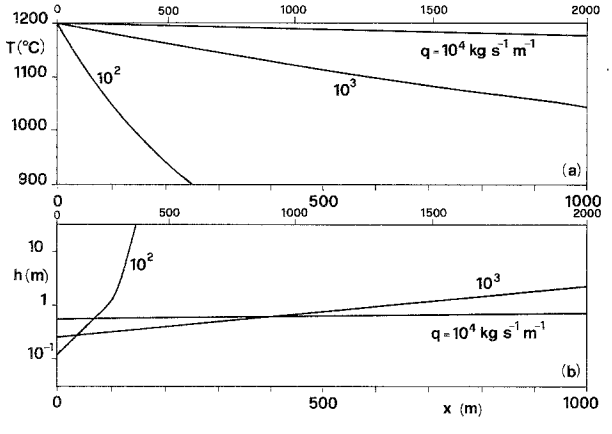

Fig. 6. Flow temperature (a) and height (b) as functions of distance x from the eruption vent, for three different values of flow rate q. The lower and upper horizontal scales refer to the thermally mixed case and to the thermally unmixed case with $T_e = 900°$ C, respectively

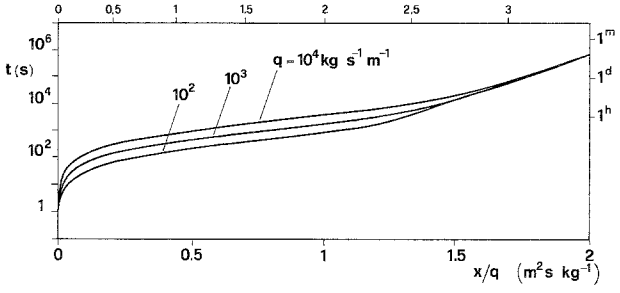

Fig. 7. Flow time t as a function of x/q, for three different values of flow rate q. The lower and upper horizontal scales refer to the thermally mixed case and to the thermally unmixed case with $T_e = 900°$ C, respectively

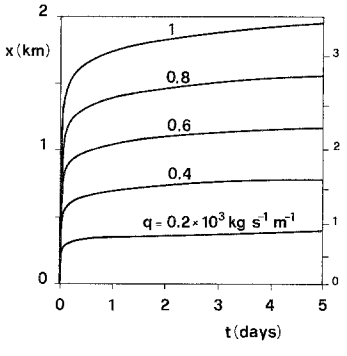

Fig. 8. Distance x from the eruption vent as a function of time t, for different values of flow rate q. The left and right vertical scales refer to the thermally mixed case and to the thermally unmixed case with $T_e = 900°$ C, respectively

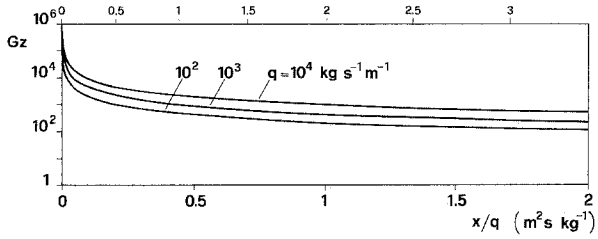

Fig. 9. Graetz number Gz along the flow, as a function of x/q, for three different values of flow rate q. The lower and upper horizontal scales refer to the thermally mixed case and to the thermally unmixed case with $T_e = 900°$ C, respectively

shows that thermal unmixing with an effective radiation temperature as high as 900° C can double the distance covered by the flow in a given time period. Actual lava flows will be of course thermally mixed close to the eruption vent and thermally unmixed downstream.

In Fig. 9 the Graetz number Gz is plotted as a function of x/q and for different values of the flow rate density. It is found empirically that the motion ceases when the value of Gz has fallen from an initially high value to a few hundred (Hulme and Fielder 1977). This value corresponds to a situation in which cooling has affected about half of the flow thickness (e.g. Hulme 1982). This observation is confirmed by the model.

Discussion and conclusions

It is not easy to compare numerical results of detailed theoretical models of lava flows with in situ observations. Measurements of lava flow parameters are in fact sparse. For instance, temperature measurements are often limited to a single point in the flow, while rheological parameters are very seldom estimated. Simultaneous measurements of several quantities, such as flow dimensions and velocity, temperature, viscosity and yield stress, taken at different points in the flow, would be necessary for a check of theoretical models.

Some data were obtained by a study of subterminal laval flows on Mt. Etna (Pinkerton and Sparks 1976), which have smaller volumes and lower effusion rates and can be studied in greater detail than large flows. At individual vents, flow depths varied from 0.2 to 2 m, velocities from 5×10^{-3} to 0.15 m s^{-1} and effusion rates from 10^{-4} to 0.2 m^3 s^{-1}. Since channel widths varied from 0.5 to 5 m, this corresponds (if the largest width corresponds to the largest flow rate) to a mass flow rate per unit width q varying from 0.6 to 1.2×10^2 kg s^{-1} m^{-1}) assuming a density $\rho = 3000$ kg m^{-3}. Effusion temperatures varied from 1070° C to 1090° C. A comparison with the case $q = 10^2$ kg s^{-1} m^{-1} of our model shows that, if $1070° > T < 1090°$ C, then h is between 0.5 and 0.7 m and v_x is between 7 and 9×10^{-2} m s^{-1} (Figs. 4 and 5). As a result of their low effusion rates, such flows were capable of flowing for only a few hundred metres. The largest individual flows had lengths of several hundred metres and flow front thickness up to several metres. The results of the model are consistent with these data.

The model presented here is, of course, a simplification of actual lava flows. It describes the laminar flow of a Bingham liquid down a uniform slope. It does not reproduce important aspects of a lava flow, such as levée formation, the change in shape of the flow and the choice of flow path, which occur in the frontal zone. Moreover, transient phases, due to a rapid change of model parameters, cannot be described.

Since the flow model is stationary, $t(x)$ is the flow time in an already formed flow, as results from its definition, and must be considered only as roughly indicative of the time required by the front to reach a distance x. However $t(x)$ reproduces a characteristic behaviour observed in actual lava flows, which show an initial rapid advance, followed by a marked deceleration (e.g. Borgia et al. 1983; Lockwood et al. 1985).

An important point is temperature variation with depth z within the flow. Both thermally mixed and unmixed conditions have been considered. In the thermally mixed model, the temperature T is an average value over the flow thickness and is representative of the temperature in the interior only as long as the thermal boundary layer is sufficiently thin. At great distances from the eruption vent, when a thick thermal boundary layer has developed at the surface of the flow, significant differences between surface and interior temperatures may arise: discrepancies up to 50°–100° C have been found in very slow lava flows (Archambault and Tanguy 1976). Some observations (e.g. Pinkerton and Sparks 1976) show that, by the time many individual lava flows come to rest, the temperature drop in the interior is less than 100° C. Accordingly, at a certain distance from the eruption vent, thermally unmixed conditions are more appropriate. However the assumptions of an effective radiation temperature T_e, which is a constant for the whole flow length, is again a crude approximation: T_e must be part of the solution of the problem and it must decrease downstream. Explicit consideration of the vertical thermal and rheological profiles in the flow is

therefore necessary for a more complete theoretical description of lava flows.

Acknowledgements. The author wishes to thank M. Bonafede, E. Boschi, F. Innocenti and D. A. Yuen for useful hints and comments on the subject of this paper. Thanks to P. Delaney for constructive comments on the first version of the manuscript. Technical help by M. Bacchetti and M. C. Jannuzzi is also acknowledged. This work has been supported by the Gruppo Nazionale per la Vulcanologia of CNR.

References

Archambault C, Tanguy JC (1976) Comparative temperature measurements on Mount Etna lavas: problems and techniques. J Volcanol Geotherm Res 1:113–125

Baloga S, Pieri D (1986) Time-dependent profiles of lava flows. J Geophys Res 91:9543–9552

Borgia A, Linneman S, Spencer D, Morales LD, Andre JB (1983) Dynamics of lava flow fronts, Arenal Volcano, Costa Rica. J Volcanol Geotherm Res 19:303–329

Daneš ZF (1972) Dynamics of lava flows. J Geophys Res 77:1430–1432

Dragoni M, Bonafede M, Boschi E (1986) Downslope flow models of a Bingham liquid: implications for lava flows. J Volcanol Geotherm Res 30:305–325

Emerman SH, Turcotte DL (1983) A fluid model for the shape of accretionary wedges. Earth Planet Sci Lett 63:379–384

Hulme G (1974) The interpretation of lava flow morphology. Geophys JR Astr Soc 39:361–383

Hulme G (1982) A review of lava flow processes related to the formation of lunar sinuous rilles. Geophys Surv 5:245–279

Hulme G, Fielder G (1977) Effusion rates and rheology of lunar lavas. Phil Trans R Soc A285:227–234

Huppert HE (1982) Flow and instability of a viscous current down a slope. Nature 300:427–429

Johnson AM (1970) Physical processes in geology. Freeman-Cooper, San Francisco

Johnson AM, Pollard DD (1973) Mechanics of growth of some laccolithic intrusions in the Henry Mountains, Utah, I. Tectonophysics 18:261–309

Landau L, Lifchitz E (1971) Méchanique des fluides. Éditions MIR, Moscow, pp 670

Lockwood JP, Banks NG, English TT, Greenland LP, Jackson DB, Johnson DJ, Koyanagi RY, McGee KA, Okamura AT, Rhodes JM (1985) The 1984 eruption of Mauna Loa Volcano, Hawaii. Eos 66:169–171

Malin MC (1980) Lengths of Hawaiian lava flows. Geology 8:306–308

McBirney AR, Murase T (1984) Rheological properties of magmas. Ann Rev Earth Planet Sci 12:337–357

McBirney AR, Noyes RM (1979) Crystallization layering of the Skaergaard intrusion. J Petrol 20:487–554

Murase T, McBirney AR (1970) Viscosity of lunar lavas. Science 167:1491–1493

Park S, Iversen JD (1984) Dynamics of lava flow: thickness growth characteristics of steady two-dimensional flow. Geophys Res Lett 11:641–644

Pieri DC, Baloga SM (1986) Eruption rate, area and length relationships for some Hawaiian lava flows, J Volcanol Geotherm Res 30:29–45

Pinkerton H, Sparks RSJ (1976) The 1975 sub-terminal lavas, Mount Etna: a case history of the formation of a compound lava field. J Volcanol Geotherm Res 1:167–182

Pinkerton H, Sparks RSJ (1978) Field measurements of the rheology of lava. Nature 276:383–385

Robson GR (1967) Thickness of Etnean lavas. Nature 216:251–252

Scarfe CM (1973) Viscosity of basic magmas at varying pressure. Nature 241:101–102

Shaw HR (1969) Rheology of basalt in the melting range. J Petrol 10:510–534

Shaw HR, Wright TL, Peck DL, Okamura R (1968) The viscosity of basaltic magma: an analysis of field measurements in Makaopuhi Lava Lake, Hawaii. Am J Sci 266:225–264

Skelland AHP (1967) Non-newtonian flow and heat transfer. Wiley, New York, pp 469

Sparks RSJ, Pinkerton H (1978) Effect of degassing on rheology of basaltic lava. Nature 276:385–386

Sparks RSJ, Pinkerton H, Hulme G (1976) Classification and formation of lava levees on Mount Etna, Sicily. Geology 4:269–271

Spera FJ, Yuen DA, Kirschvink SJ (1982) Thermal boundary layer convection in silicic magma chambers: effects of temperature-dependent rheology and implications for thermogravitational chemical fractionation. J Geophys Res 87:8755–8767

Wadge G (1978) Effusion rate and the shape of aa lava flowfields on Mount Etna. Geology 6:503–506

Walker GPL (1967) Thickness and viscosity of Etnean lavas. Nature 213:484–485

Walker GPL (1973) Lengths of lava flows, Philos. Trans R Soc A 274:107–118

Wilson L, Head JW III (1983) A comparison of volcanic eruption processes on Earth, Moon, Mars, Io and Venus. Nature 302:663–669

Received June 23, 1988/Accepted September 16, 1988